

Cite this: DOI: 00.0000/xxxxxxxxxx

A nanofluidic exchanger for harvesting saline gradients energy- Supplementary Information

Saranath Sripriya,^a Cyril Picard,^a Vincent Larrey,^b Frank Fournel,^b and Elisabeth Charlaix^{*a}

1 One-dimensional Poisson-Nernst-Planck equation with ions of different diffusivities

We follow the derivation of section 3.1 of the main text, considering that the cations and anions have a different diffusion coefficient respectively D^+ and D^- . In these conditions the transport equations (1a) and (1b) of section 3.1 become:

$$J^+ = -D^+H \left(\frac{dc^+}{dx} + c^+ \frac{d\psi}{dx} \right) \quad (1a)$$

$$J^- = -D^-H \left(\frac{dc^-}{dx} - c^- \frac{d\psi}{dx} \right) \quad (1b)$$

while equation (1c) remains the same. Introducing the reduced coordinates $\bar{x} = x/W$, the reduced concentrations $\tilde{c}^\pm = c^\pm eH/|\sigma|$, the average concentration $\tilde{c} = (\tilde{c}^+ + \tilde{c}^-)/2$, and the reduced fluxes $K^{+,-} = eWJ^\pm/|\sigma|D^\pm$, the 1D-PNP equations become:

$$\frac{eW}{|\sigma|} \left(\frac{J^+}{D^+} + \frac{J^-}{D^-} \right) = K^+ + K^- = -2 \left(\frac{d\tilde{c}}{d\bar{x}} + \frac{d\psi}{d\bar{x}} \right) \quad (2a)$$

$$\frac{eW}{|\sigma|} \left(\frac{J^+}{D^+} - \frac{J^-}{D^-} \right) = K^+ - K^- = - \left(2\tilde{c} \frac{d\psi}{d\bar{x}} \right) \quad (2b)$$

These equations in K^+ , K^- , \tilde{c} and ψ are exactly the same as equations (2) of the main text, and therefore the modified selectivity $\eta = (K^+ - K^-)/(K^+ + K^-)$ replaces ι in equation (3a) while (3b) is unchanged.

As boundary condition we assume the continuity of the non-dimensional electrochemical potential of the anions and cations, respectively $\ln c^+ + \psi$ and $\ln c^- - \psi$, at $x = 0$ and $\bar{x} = 1$. With an electrolyte concentration c_{ho} at the level of the nanoslit in the high concentration nanoduct and a reduced potential ψ_h , the boundary conditions at $\bar{x} = 0$ write:

$$\begin{aligned} \ln \tilde{c}_{ho} \pm \psi_h &= \ln \tilde{c}^\pm(0^+) \pm \psi(0^+) \\ \tilde{c}^+(0^+) \tilde{c}^-(0^+) &= \tilde{c}_{ho}^2 \quad \psi_h = \frac{1}{2} \ln \frac{\tilde{c}^+(0^+)}{\tilde{c}^-(0^+)} + \psi(0^+) \end{aligned} \quad (3)$$

Together with the charge balance in the nanoslit (equation (1c) of the main text) $\tilde{c}^+(0^+) - \tilde{c}^-(0^+) = -2\text{sgn}(\sigma)$, the anion and cation concentrations at entrance of the nanoslit are:

$$\tilde{c}^\pm(0^+) = \mp \text{sgn}(\sigma) + \sqrt{1 + \tilde{c}_{ho}^2} \quad (4)$$

Thus the reduced electrolyte concentration \mathcal{C}_h at the entrance of the nanoslit is:

$$\mathcal{C}_h = \frac{\tilde{c}^+(0^+) + \tilde{c}^-(0^+)}{2} = \sqrt{1 + \tilde{c}_{ho}^2} = \sqrt{1 + (\tilde{c}_{ho}eH/\sigma)^2}$$

The same relation holds between \mathcal{C}_ℓ and $\tilde{c}_{\ell o}$ at the outlet of the nanoslit $\bar{x} = 1^-$, and these relations constitute equation (4a) of the main text. The relation between $\psi(1^-)$ and ψ_ℓ is the analogous of equation (3) at $\bar{x} = 1$, so that :

$$\begin{aligned} \psi(1^-) - \psi(0^+) &= \psi_\ell - \psi_h + \frac{1}{2} \ln \frac{\tilde{c}^+(0^+) \tilde{c}^-(1^-)}{\tilde{c}^-(0^+) \tilde{c}^+(1^-)} \\ \psi(1^-) - \psi(0^+) &= \Delta\psi + \ln \frac{\tilde{c}_{\ell o}(\mathcal{C}_h - \text{sgn}(\sigma))}{\tilde{c}_{ho}(\mathcal{C}_\ell - \text{sgn}(\sigma))} \end{aligned} \quad (5)$$

With $\Delta\psi = \psi_\ell - \psi_h$ and $\sigma < 0$ this is equation (4b) of the main text.

The modified selectivity $\eta = (K^+ - K^-)/(K^+ + K^-)$ replaces ι in equation (5a):

$$\eta \ln \frac{\mathcal{C}_h - \eta}{\mathcal{C}_\ell - \eta} + \mathcal{C}_h - \mathcal{C}_\ell = -\Delta\psi + \mathcal{E} \quad (6)$$

while \mathcal{E} is given by the unchanged equation (5b). Equation (6a) becomes:

$$K^\pm = (1 \pm \eta)(-\Delta\psi + \mathcal{E}) \quad (7)$$

from which one get the cations and anions fluxes and the electrical current:

$$J^\pm = \frac{D^\pm |\sigma|}{eW} (1 \pm \eta)(-\Delta\psi + \mathcal{E}) \quad (8)$$

$$dI = \frac{2D|\sigma|}{W} (\xi + \eta)(-\Delta\psi + \mathcal{E}) \quad (9)$$

Finally in order to recover the selectivity ι one introduces the av-

^a Université Grenoble Alpes, CNRS, LiPhy, 38000 Grenoble France.

* E-mail: elisabeth.charlaix@univ-grenoble-alpes.fr

^b CEA-Leti: Laboratoire d'électronique des technologies de l'information, 17 Avenue de Martyrs 38054 Grenoble.

† Electronic Supplementary Information (ESI) available: [details of any supplementary information available should be included here]. See DOI: 00.0000/00000000.

erage diffusion and diffusion contrast:

$$D = \frac{D^+ + D^-}{2} \quad \xi = \frac{D^+ - D^-}{D^+ + D^-} \quad (10)$$

$$t = \frac{J^+ - J^-}{J^+ + J^-} = \frac{\eta + \xi}{\eta\xi + 1} \quad (11)$$

When the ions diffusivity are equal, $\xi = 0$ and $t = \eta$, and the expressions reduce to the one of the main text.

2 Optimizing the net power in the 1D-approximation of the exchanger

Starting from eq (15) in the main text

$$\mathcal{P}_{net} = \frac{k_B T D |\sigma|}{e W b} \left(f - \frac{K D \eta e H^2 L^2}{2 k_B T |\sigma| W b^4} S h^2 \right) \quad (12)$$

we search for the exchanger parameters which maximize the net extractable power density for fixed chemical conditions (i.e surface charge, salinity, solutions viscosity, diffusion coefficient, temperature). We optimize the geometric parameters by keeping constant the ratio $L/b = \lambda$. Using the relation $H = |\sigma| / (e C_H D u_H)$ we introduce the fixed volume and power

$$\mathcal{V} = \frac{K D \eta |\sigma|}{k_B T e C_H^2} \quad \tilde{P} = \frac{k_B T D |\sigma|}{e} \quad (13)$$

so that

$$\mathcal{P}_{net} = \frac{\tilde{P}}{W b} \left(f - \frac{\mathcal{V} \lambda^2}{2 W b^2} \left(\frac{Sh}{Du_H} \right)^2 \right) \quad (14)$$

the power \tilde{P} is equal to 16 pW for a surface charge $|\sigma| = 0.64 \text{ C/m}^2$ at ambient temperature. The non-dimensional power factor f is a function of non-dimensional numbers only, and therefore does not depend on the specific value of b . There is thus an optimum value of b corresponds to $\partial \mathcal{P}_{net} / \partial b = 0$ at fixed f :

$$b_{opt} = \frac{Sh}{Du_H} \sqrt{\frac{3 \mathcal{V} \lambda^2}{2 W f}} \quad (15)$$

With this optimum value the net power becomes

$$\mathcal{P}_{net} = \frac{2\sqrt{2}}{3\sqrt{3}} \frac{\tilde{P}}{\sqrt{W \mathcal{V} \lambda^2}} \frac{Du_H}{Sh} f^{3/2} \quad (16)$$

which corresponds to a ratio between the produced electrical power and the dissipated hydraulic power equal to 3, and consequently a net power twice larger than the dissipated power.

The maximum net power is reached when $\tilde{f}^{3/2} Du_H / Sh$ is maximum. This maximum is expected to be found at a value of Sherwood large enough ($Sh / Du_H > 5$) so that the empirical master law (14a) reduces to

$$f \approx f \left(\frac{Sh}{Du_H} = y \right) = \frac{1}{4} W_0(y e^2) \left(W_0((y+2)e^2) - 2 \right)$$

where W_0 is the principal branch of the Lambert W function. In this framework $\tilde{f}^{3/2} Du_H / Sh$ is a function of the single variable $y = Sh / Du_H$. It has a maximum at $Sh / Du_H = 14.83$ of value

$\tilde{f}^{3/2} Du_H / Sh = 0.1050$, corresponding to $f = 1.34$. Consequently

$$b_{opt} = 15.7 \lambda \sqrt{\frac{\mathcal{V}}{W}} \quad (17)$$

$$\mathcal{P}_{net,max} = 0.057 \frac{\tilde{P}}{\lambda \sqrt{W \mathcal{V}}} \quad (18)$$

It is worth to note that the prefactor 15.7 and 0.057 come exclusively from the mathematical properties of the master function (17), and are independant of the values of chemical, flow, or geometrical parameters. Replacing \mathcal{V} and \tilde{P} by there respective expression one gets

$$b_{opt} = 15.7 \frac{\lambda}{C_H} \sqrt{\frac{K D \eta |\sigma|}{W k_B T e}} \quad (19)$$

$$\mathcal{P}_{net,max} = 0.057 \frac{C_H}{\lambda} \sqrt{\frac{(k_B T)^3 D |\sigma|}{W K \eta e}} \quad (20)$$

In this optimal configuration, the optimal average velocity U_{opt} for nanoducts of square section (corresponding to $K = 7.1$) is

$$U_{opt} = \frac{Sh D H L}{2 W b_{opt}^2} = \frac{1}{2} \sqrt{\frac{D |\sigma| k_B T}{K \eta W e}}$$

It is worth noting that the only geometrical variable which impacts this optimal velocity is W . The pressure difference ΔP_{opt} between the entry and the exit of one nanoduct of the elemental converter is consequently

$$\Delta P_{opt} = K \eta \frac{U_{opt} \lambda}{b_{opt}} = 0.0321 k_B T C_H \quad (21)$$

It is a quite remarkable fact, that once the exchanger is designed with $a = b = b_{opt}$, the pressure needed to reach the maximum net harvested pressure depends only on the osmotic pressure of the high salinity solution, and not other parameters. At ambient temperature, for a square microchannel, $D = 10^{-9} \text{ m}^2/\text{s}$, $\eta = 10^{-3} \text{ Pas.s}$, $|\sigma| = 0.64 \text{ C/m}^2$, and sea water salt concentration $C_H = 0.6 \text{ M}$, $\mathcal{V} = 44 \text{ nm}^3$ while for a reference concentration $C_0 = 1 \text{ M}$, $\mathcal{V}_0 = 16 \text{ nm}^3$. The last volume is useful to be able to estimate easily b_{opt} and \mathcal{P}_{max} for different solute concentration as

$$b_{opt} = 15.7 \frac{C_0}{C_H} \lambda \sqrt{\frac{\mathcal{V}_0}{W}} \quad (22)$$

$$\mathcal{P}_{max} = 0.057 \frac{C_H}{C_0} \frac{\tilde{P}}{\lambda \sqrt{W \mathcal{V}_0}} \quad (23)$$

3 Asymptotic behaviour of \mathcal{P}_{elec} at small and large Sherwood

In the 1D-approximation of the Elemental Exchanger, the general advection diffusion equations in the high and low concentrations microchannels are give by equation (12) of the main text that we

rewrite as:

$$\frac{1}{Pe} \frac{\partial^2 \bar{c}_h}{\partial \bar{z}^2} - \frac{\partial \bar{c}_h}{\partial \bar{z}} - \frac{(1+t)}{Sh} (\mathcal{E} - \Delta\psi) = 0 \quad (24a)$$

$$\frac{1}{Pe} \frac{\partial^2 \bar{c}_l}{\partial \bar{z}^2} - \frac{\partial \bar{c}_l}{\partial \bar{z}} + \frac{(1+t)}{Sh} (\mathcal{E} - \Delta\psi) = 0 \quad (24b)$$

with $\bar{c}_{h,l} = c_{h,l}eH/|\sigma|$, t and \mathcal{E} given by eqs (4a, 5a) and (5b) of the main text. The sum and difference leads to diffusion-convection equations for $\bar{c}_d = \bar{c}_h - \bar{c}_l$ and $\bar{c}_s = \bar{c}_h + \bar{c}_l$

$$\frac{1}{Pe} \frac{\partial^2 \bar{c}_s}{\partial \bar{z}^2} - \frac{\partial \bar{c}_s}{\partial \bar{z}} = 0 \quad (25a)$$

$$\frac{1}{Pe} \frac{\partial^2 \bar{c}_d}{\partial \bar{z}^2} - \frac{\partial \bar{c}_d}{\partial \bar{z}} = 2 \frac{(1+t)}{Sh} (\mathcal{E} - \Delta\psi) \quad (25b)$$

It is clear that the only solution of the first equation satisfying both the boundary condition at the inlet ($-\partial_z \bar{c}_s / Pe + \bar{c}_s = \bar{c}_H + \bar{c}_L$) and at the outlet ($\partial_z \bar{c}_s = 0$) is $\bar{c}_s(z) = \bar{c}_s = \bar{c}_H + \bar{c}_L$.

We simplify (25b) by introducing the functions:

$$\varphi = \bar{c}_d - \frac{1}{Pe} \frac{\partial \bar{c}_d}{\partial z} \quad \mathcal{U} = \mathcal{E} - \Delta\psi \quad (26)$$

so that equation (25b) rewrites

$$\frac{\partial \varphi}{\partial \bar{z}} = -\frac{2}{Sh} (1+t) \mathcal{U} \quad (27)$$

and the dimensionless electrical power per unit surface is

$$\begin{aligned} \mathcal{P}_{elec} &= \Delta\psi \int_0^1 t \mathcal{U} d\bar{z} \\ &= \Delta\psi \left(-\frac{Sh}{2} \int_{\varphi_m}^{\varphi_{out}} d\varphi - \int_0^1 \mathcal{U} d\bar{z} \right) \end{aligned} \quad (28)$$

In order to find the limit behaviours at small and large Sherwood, we proceed to some approximations. A first approximation takes into account that $\mathcal{E}_{h,l}$ are close to unity and can be expanded as:

$$\mathcal{E}_{h,l} \simeq 1 + \frac{1}{2} \bar{c}_{h,l}^2 \quad \mathcal{E}_h - \mathcal{E}_l \simeq \frac{\bar{c}_s \bar{c}_d}{2} \quad (29)$$

This is because the reduced concentrations \bar{c}_h and \bar{c}_l are always smaller than unity, therefore the approximation (29) is always satisfied within 10%.

A second approximation involves the selectivity t :

$$t \sim 1 - \frac{\bar{c}_s \bar{c}_d}{2\mathcal{U}} \quad (30)$$

The above relation is established by using the change of variable (55) and writing eq. (56) as

$$v \left((\mathcal{E}_h - \mathcal{E}_l) \left(\coth(v) - \frac{1}{v} \right) + \mathcal{E}_h + \mathcal{E}_l \right) = 2vt - \mathcal{E}_h + \mathcal{E}_l = -\mathcal{U}$$

In the operation condition of the exchanger, v cannot be very large because this would require a very large $\Delta\psi$ and a negative harvested power. Due to the fact that $\mathcal{E}_h - \mathcal{E}_l \ll \mathcal{E}_h + \mathcal{E}_l$, the solution in v of the above equation is thus $v \simeq -\mathcal{U}/(\mathcal{E}_h + \mathcal{E}_l)$. Using the

expansion of eq. (29) for $\mathcal{E}_h, \mathcal{E}_l$ we get the approximation (30).

Injecting (30) in (27) we get an expression for \mathcal{U} :

$$\frac{\partial \varphi}{\partial \bar{z}} = -\frac{2}{Sh} \left(2 - \frac{\bar{c}_s \bar{c}_d}{2\mathcal{U}} \right) \mathcal{U} = -\frac{4\mathcal{U}}{Sh} + \frac{\bar{c}_s \bar{c}_d}{Sh} \quad (31)$$

$$\mathcal{U} = -\frac{Sh}{4} \left(\frac{\partial \varphi}{\partial \bar{z}} - \frac{\bar{c}_s \bar{c}_d}{Sh} \right)$$

from which the electrical power harvested writes

$$\frac{\mathcal{P}_{elec}}{\Delta\psi} = -\frac{Sh}{4} \int_{\varphi_m}^{\varphi_{out}} d\varphi - \int_0^1 \frac{\bar{c}_s \bar{c}_d}{4} dz \quad (32)$$

Low Sherwood. At low Sherwood number, the concentration difference drops rapidly downstream of the injection point, and reaches a uniform profile \bar{c}_d^* when the exchange between the nanochannels vanishes. This is obtained when the selectivity reaches the value $t = -1$, for which the r.h.s. of (27) vanishes. According to the implicit equation (52,53) satisfied by t , one sees that the condition $t = -1$ corresponds to:

$$\ln \frac{\bar{c}_h^*}{\bar{c}_l^*} = \Delta\psi \quad (33)$$

whereby we get the expression of \bar{c}_d^*

$$\bar{c}_d^* = \bar{c}_s \frac{e^{\Delta\psi} - 1}{e^{\Delta\psi} + 1} \quad (34)$$

As the concentration profile is flat at the outlet, $\varphi^{out} = c_d^*$. Furthermore, the lowest is Sherwood, the shortest is the nanochannel portion where \bar{c}_d is significantly different from \bar{c}_d^* . Therefore in the low Sherwood limit the electrical power writes:

$$\mathcal{P}_{elec} \simeq \Delta\psi \left(\frac{Sh}{4} (\bar{c}_D - c_d^*) - \frac{\bar{c}_s \bar{c}_d^*}{4} \right) \quad (35)$$

where $\bar{c}_D = \bar{c}_H - \bar{c}_L$ is the inlet flux. Because Sherwood is low, the value of the electrical potential difference $\Delta\psi_{max}$ giving the maximum value of the power is significantly smaller than 1, and $\bar{c}_d^* \simeq \bar{c}_s \Delta\psi / 2$. In these conditions the exchanger behaves like a linear generator, and the maximum electrical power (35) is obtained at $\Delta\psi_{max} = Sh \bar{c}_D / \bar{c}_s^2$ and has the value

$$\mathcal{P}_{elec,max} \simeq \frac{Sh^2 \bar{c}_D^2}{8 \bar{c}_s^2} \quad (36)$$

When the inlet salinity ratio is significant, we recover the behaviour in $Sh^2/8$.

Large Sherwood. We start from equation (32) for the power. As we expect to find a power growing with Sh at high Sherwood, we neglect the 2nd term of the r.h.s, which is always bounded by the value $\bar{c}_s^2/4$. Thus equation (32) is simplified in:

$$\mathcal{P}_{elec} \simeq \Delta\psi \frac{Sh}{4} (\varphi^{in} - \varphi^{out}) \quad (37)$$

Second, we take into account that at high Sherwood the diffusive term in eq. (26) is negligible and convection dominates. This leads to $\varphi \simeq \bar{c}_d$.

Equation (31) is then used to find the variation of φ between

the inlet and the outlet of the nanochannels. Injecting in (31) the expression of \mathcal{U} obtained from the developments of $\mathcal{C}_h, \mathcal{C}_l$ (eq. 29):

$$\mathcal{U} \simeq \ln \frac{\bar{c}_h}{\bar{c}_l} + \frac{\bar{c}_s \bar{c}_d}{4} - \Delta\psi$$

one get:

$$\begin{aligned} \frac{\partial \varphi}{\partial z} &= -\frac{4}{Sh} \left(\ln \frac{\bar{c}_h}{\bar{c}_l} - \Delta\psi \right) \\ &\simeq -\frac{4}{Sh} \left(\ln \frac{\bar{c}_s + \varphi}{\bar{c}_s - \varphi} - \Delta\psi \right) \end{aligned} \quad (38)$$

We note that the variation of φ is not very large at high Sh , therefore φ remains more or less close to its initial value $\varphi^{in} = \bar{c}_D$. We introduce the new function

$$\varepsilon = \frac{(\bar{c}_s - \varphi)e^{\Delta\psi}}{2\bar{c}_s} \quad \varphi = \bar{c}_s(1 - 2e^{-\Delta\psi}\varepsilon) \quad (39)$$

so that the previous equation writes :

$$-2\bar{c}_s e^{-\Delta\psi} \frac{\partial \varepsilon}{\partial z} = \frac{4}{Sh} \left[\ln \varepsilon - \ln(1 - e^{-\Delta\psi}\varepsilon) \right] \quad (40)$$

The inlet value of ε is $\varepsilon^{in} = e^{\Delta\psi}/2(1 + Cr)$ where $Cr = \bar{c}_H/\bar{c}_L$ is the inlet concentration ratio. For $Cr > 10$ the inlet value verifies $\varepsilon^{in} e^{-\Delta\psi} \ll 1$. We assume in the following, and verify at the end of the calculation, that the condition $\varepsilon e^{-\Delta\psi} \ll 1$ is met for all z at the value $\Delta\psi_{max}$ for which the power is maximum. In these conditions the r.h.s. of (40) is dominated by its first term. For the sake of simplicity, but this does not change the final result, we neglect the 2nd term so that (40) writes:

$$\frac{d\varepsilon}{\ln \varepsilon} = -\frac{2e^{\Delta\psi}}{\bar{c}_s Sh} dz \quad (41)$$

which integrates in

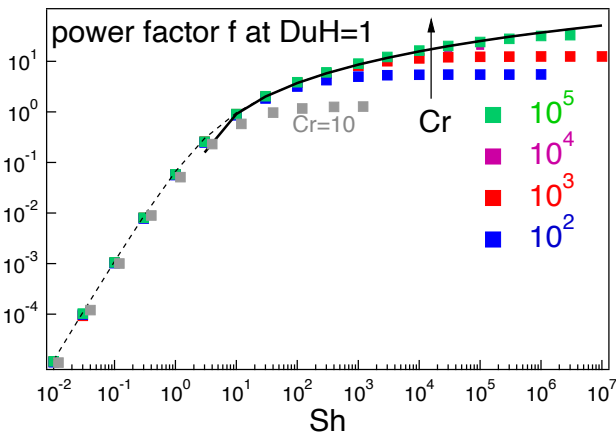


Fig. 1 Points of the Fig.3 of the main paper complemented with asymptotic expressions 36 (dashed line) and 49 for $Du_H = 11$ and for $\varepsilon_{in} \rightarrow 0$ (thick line).

$$\text{Ei}[\ln(\varepsilon^{out})] - \text{Ei}[\ln(\varepsilon^{in})] = -\frac{2e^{\Delta\psi}}{\bar{c}_s Sh} \quad (42)$$

where Ei is the exponential integral function. We then focus to the envelope of the power curves when the concentration ratio becomes very large, that is $\varepsilon^{in} = 0$. This leads to the expression for the power:

$$\text{Ei}[\ln(\varepsilon^{out})] = -\frac{2e^{\Delta\psi}}{\bar{c}_s Sh} \quad (43)$$

$$\mathcal{P}_{elec} = \frac{\Delta\psi \varepsilon^{out}}{-\text{Ei}[\ln(\varepsilon^{out})]} \quad (44)$$

The maximum power is obtained when $d\mathcal{P}_{elec}/d(\Delta\psi) = 0$. By taking the derivative of equations (43):

$$\frac{d\text{Ei}[\ln(\varepsilon^{out})]}{d(\Delta\psi)} = \text{Ei}[\ln(\varepsilon^{out})] = \frac{1}{\ln \varepsilon^{out}} \frac{d\varepsilon^{out}}{d(\Delta\psi)}$$

and the derivative of (44), we get a relation for the value $\Delta\psi_{max}$ at which the power is maximum:

$$\frac{\Delta\psi_{max} - 1}{\Delta\psi_{max}} = \frac{\ln \varepsilon^{out}}{\varepsilon^{out}} \text{Ei}[\ln(\varepsilon^{out})] \quad (45)$$

Expanding the above equation to the first order in $1/\ln \varepsilon^{out}$ we get the expression of $\Delta\psi_{max}$:

$$\frac{\Delta\psi_{max} - 1}{\Delta\psi_{max}} \simeq 1 + \frac{1}{\ln \varepsilon^{out}} \quad \Delta\psi_{max} = -\ln \varepsilon^{out} \quad (46)$$

where terms in $1/(\ln \varepsilon^{out})^2 \simeq 1/(\Delta\psi_{max})^2$ have been neglected. Injecting this value of $\Delta\psi_{max}$ in (43) with an expansion at the same order we get:

$$\text{Ei}(-\Delta\psi_{max}) \simeq -\frac{e^{-\Delta\psi_{max}}}{\Delta\psi_{max}} \left(1 - \frac{1}{\Delta\psi_{max}} \right) = -\frac{2e^{\Delta\psi_{max}}}{\bar{c}_s Sh}$$

that writes, neglecting the terms in $1/(\Delta\psi_{max})^2$, as:

$$e^{2\Delta\psi_{max}+2}(2\Delta\psi_{max}+2) = e^2 \bar{c}_s Sh \quad (47)$$

The above equation solves as:

$$\Delta\psi_{max} = \frac{1}{2} W_0 \left(e^2 \bar{c}_s Sh \right) \quad (48)$$

$$\mathcal{P}_{elec,max} = f = \frac{1}{4} W_0(e^2 \bar{c}_s Sh) \left(W_0(e^2 \bar{c}_s Sh) - 2 \right) \quad (49)$$

where the function W_0 is the Lambert function, that is the reciprocal of xe^x .

At high concentration ratio, the argument $\bar{c}_s Sh$ becomes Sh/Du_H .

Equation (49) describes the asymptotic expansion of the maximum electric power at $Sh/Du_H \geq 2$ for an infinitely large initial salinity ratio $Cr = c_H/c_L = \infty$. We see on figure 3, that this asymptotic expansion actually describes very well all salinity ratios $Cr > 10$, up to the Sherwood value for which the (adimensional) power saturates to the value $\mathcal{F}(Du_H, Du_L)$.

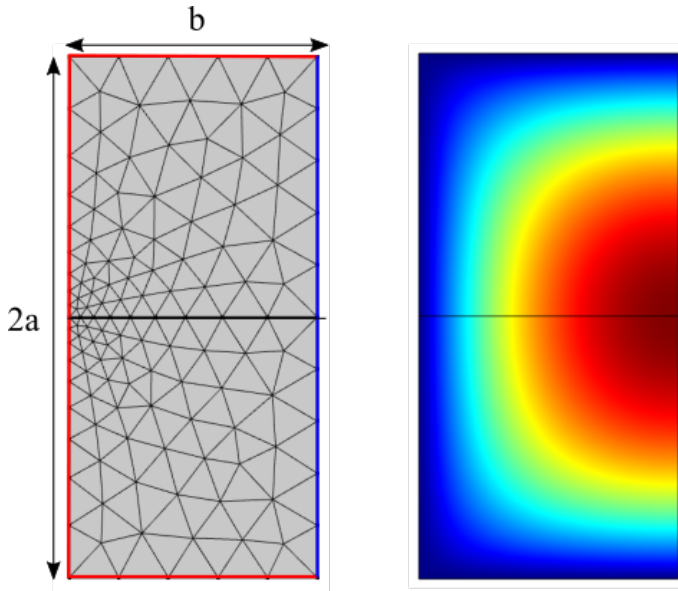


Fig. 2 Simulation geometry and mesh configuration (left) and the resulting velocity profile (right) calculated inside the microchannel section in arbitrary units. In the simulation geometry (left) the red borders correspond to zero velocity and the blue border corresponds to zero flux condition.

4 Modelling the Elemental Exchanger using COMSOL Multiphysics

The 3D transport equations of the electrolyte in the microchannels (Eqs 3 of the article) were implemented in the COMSOL software using the *Equation-based modelling* feature of COMSOL, and more specifically the *General Form Partial Differential Equations* which solves conservative equations of the form

$$\vec{\nabla} \cdot \vec{\Gamma} = s \quad (50)$$

well-suited for a diffusion-convection equation.

As the convective velocity $u(x,y)\vec{e}_z$ is invariant along the z -direction, a velocity template $\tilde{u}(x,y)$ in the half-microchannel section of with b (x -axis) and height $2a$ (y -axis) was first calculated separately by solving the Stokes equation $\vec{\nabla} \cdot \vec{\nabla} \tilde{u} = Cte$ in the section, and then rescaled so that $\iint \tilde{u}(x,y) dx dy = 2ab$. The 3D-transport equations were then solved in the microchannels for various average velocity U and applied potential $\Delta\psi$, by using this template multiplied by the targeted velocity U .

The mesh of the section was refined around the point corresponding to the location of the nanoslit, as shown in Figure (2). This 2D-mesh was further taken as the source of the 3D-domain mesh obtained by sweeping it in the z -direction (see Figure 2). It was checked that a mesh size around the nanoslit of less than $5 \cdot 10^{-2}b$ did not change the overall numerical results.

The 3D convection-diffusion equation (3) were solved on a block of section $2ab$ extending from $z = -0.05 * L$ up to L . The additional block $-0.05 * L \leq z \leq 0$ was added to the active part $z \in [0, L]$ in order to allow upstream diffusion of the concentration at low velocity. The equations were solved on this domain for the

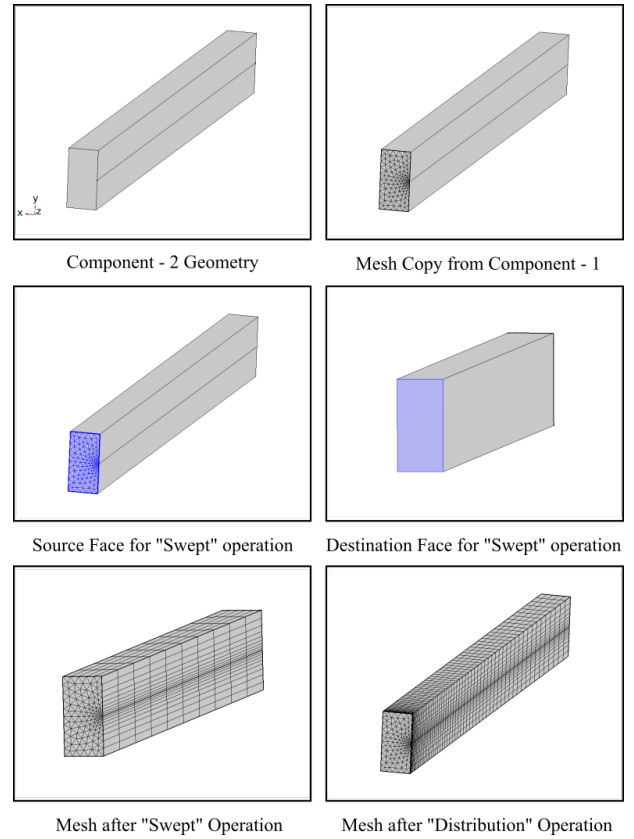


Fig. 3

two normalized concentration fields $\tilde{c}_{h,l} = eHc_{h,l}/|\sigma|$, written as

$$\begin{aligned} \vec{\nabla} \cdot \left(-\vec{\nabla} \tilde{c}_{h,l} + \frac{U}{D} \tilde{u} \tilde{c}_{h,l} \vec{e}_z \right) = \\ \pm \frac{H}{W} (1+t) (-\Delta\psi + \mathcal{E}) \delta(x,y) \end{aligned} \quad (51)$$

A unique diffusion coefficient D was assumed for anions and cations, of value $D = 10^{-9} m^2/s$.

The inlet boundary condition at $z = 0.05L$ was a prescribed flux:

$$-\vec{\nabla} \tilde{c}_{h,l} + \frac{U}{D} \tilde{u}(x,y) \tilde{c}_{h,l} = \frac{U}{D} \tilde{u}(x,y) \tilde{c}_{H,L}$$

and the outlet boundary condition at $z = L$ was a purely convective flux

$$-\vec{\nabla} \tilde{c}_{h,l} = 0 \quad z = L$$

The r.h.s. was implemented using the *Edge source* feature of COMSOL on an edge running from $z = 0$ to $z = L$ located at half-height of the domain. For this purpose, the variables \mathcal{E} and t (Eq. (12) and (14)) had to be calculated on this edge:

$$\mathcal{E} = \ln \frac{\tilde{c}_h}{\tilde{c}_l} + \mathcal{C}_h - \mathcal{C}_l - \ln \frac{\mathcal{C}_h + 1}{\mathcal{C}_l + 1} \quad (52)$$

$$t \ln \frac{\mathcal{C}_h - t}{\mathcal{C}_l - t} + \mathcal{C}_h - \mathcal{C}_l = \Delta\psi - \mathcal{E} \quad (53)$$

$$\mathcal{C}_{h,l} = \sqrt{1 + \tilde{c}_{h,l}^2} \quad (54)$$

(with $\eta = t$ and $\xi = 0$). This was done using the *Edge ODEs and DAEs* feature of *COMSOL* for solving algebraic equations. Note that the algebraic equation 53 was not solved as such, but transformed using the variable change:

$$v = \frac{1}{2} \ln \frac{\mathcal{C}_h - t}{\mathcal{C}_l - t} \quad t = \frac{\mathcal{C}_h - \mathcal{C}_l}{2 \tanh(v)} + \frac{\mathcal{C}_h + \mathcal{C}_l}{2} \quad (55)$$

and we solve the equation in v :

$$v \left((\mathcal{C}_h - \mathcal{C}_l) \left(\coth(v) - \frac{1}{v} \right) + \mathcal{C}_h + \mathcal{C}_l \right) = \Delta\psi - \mathcal{E} \quad (56)$$

admitting a single solution in v for all values of the r.h.s.

The mesh of the 3D domain (Figure 3) was constructed by sweeping the mesh of the 2D section in the z -direction. It was found that the resolution in z at the upstream extremity of the edge source $z = 0$ was of particular importance, as concentration polarization at this level is low and the region provides a high contribution to the total current. An evolutive mesh size of 60 elements along the z -direction with the first element thickness equal to $10^{-3}L$ was used, and further mesh refinement did not change significantly the results.